Cardiovascular Research (2010) **85**, 739–750
doi:10.1093/cvr/cvp345

Complete loss of murine Xin results in a mild cardiac phenotype with altered distribution of intercalated discs

Julia Otten[1], Peter F.M. van der Ven[1,2], Padmanabhan Vakeel[1,2†], Stefan Eulitz[1], Gregor Kirfel[1], Oliver Brandau[3‡], Michael Boesl[3¶], Jan W. Schrickel[4], Markus Linhart[4], Katrin Hayeß[2§], Francisco J. Naya[5], Hendrik Milting[6], Rainer Meyer[7]*, and Dieter O. Fürst[1,2]*

[1]Department of Molecular Cell Biology, Institute for Cell Biology, University of Bonn, Ulrich-Haberland-Str. 61a, Bonn D-53121, Germany; [2]Department of Cell Biology, University of Potsdam, Potsdam, Germany; [3]Max Planck Institute for Biochemistry, Martinsried, Germany; [4]Department of Medicine-Cardiology, University of Bonn, Bonn, Germany; [5]Department of Biology, Boston University, Boston, MA 02215, USA; [6]Herz- und Diabeteszentrum NRW, Erich und Hanna Klessmann-Institut für Kardiovaskuläre Forschung und Entwicklung, Bad Oeynhausen, Germany; and [7]Institute of Physiology II, University of Bonn, Wilhelmstr. 31, Bonn, Germany

Received 2 May 2009; revised 10 August 2009; accepted 14 October 2009; online publish-ahead-of-print 19 October 2009

Time for primary review: 39 days

Aims Xin is a striated muscle-specific F-actin binding protein that has been implicated in cardiomyopathies. In cardiomyocytes, Xin is localized at intercalated discs (IDs). Mice lacking only two of the three Xin isoforms (XinAB$^{-/-}$ mice) develop severe cardiac hypertrophy. To further investigate the function of Xin variants in the mammalian heart, we generated XinABC$^{-/-}$ mice deficient in all Xin isoforms.

Methods and results XinABC$^{-/-}$ mice showed a very mild phenotype: heart weight, heart weight to tibia length ratios, and cardiac dimensions were not altered. Increased perivascular fibrosis was only observed in hearts of young XinABC$^{-/-}$ mice. Striking differences were revealed in isolated cardiomyocytes: XinABC$^{-/-}$ cells demonstrated a significantly increased number of non-terminally localized ID-like structures. Furthermore, resting sarcomere length was increased, sarcomere shortening, peak shortening at 0.5–1 Hz, and the duration of shortening were decreased, and shortening and relengthening velocities were accelerated at frequencies above 4 Hz in XinABC$^{-/-}$ cardiomyocytes. ECG showed a significantly shorter HV interval and a trend towards shorter QRS interval in XinABC$^{-/-}$ mice, suggesting a faster conduction velocity of the ventricular-specific conduction system. In human cardiac tissue, expression of XinC protein was detected solely in samples from patients with cardiac hypertrophy.

Conclusion Total Xin deficiency leads to topographical ID alterations, premature fibrosis and subtle changes in contractile behaviour; this is a milder cardiac phenotype than that observed in XinAB$^{-/-}$ mice, which still can express XinC. Together with the finding that XinC is detected solely in cardiomyopathic human tissues, this suggests that its expression is responsible for the stronger dominant phenotype in XinAB$^{-/-}$ mice. Furthermore, it indicates that XinC may be involved in the development of human cardiac hypertrophy.

Keywords Cardiac hypertrophy • Intercalated disc • Xin-repeat protein isoforms • Alternative splicing • Null mutation

† Present address. Department of Neuromuscular and Cardiovascular Cell Biology, Max-Delbrück-Center, Berlin, Germany.

‡ Present address. Institute for Physiology, Ludwig-Maximilians-University of Munich, Germany.

¶ Present address. Max Planck Institute of Neurobiology, Transgenic Service, Martinsried, Germany.

§ Present address. Bundesinstitut für Risikobewertung - ZEBET, Berlin, Germany.

* Corresponding author. Tel: +49 228 73 5301 (D.O.F.)/+49 228 287 22311 (R.M.), Fax: +49 228 73 5302 (D.O.F.)/+49 228 287 22313 (R.M.), Email: dfuerst@uni-bonn.de (D.O.F.)/rainer.meyer@ukb.uni-bonn.de (R.M.)

1. Introduction

Xin actin-binding repeat-containing proteins (XIRPs) are a family of striated muscle-specific proteins characterized by 16 amino acids Xin repeats that bind F-actin.[1,2] The first protein containing these repeats was detected in chicken embryos, and because of its strong cardiac expression, named 'Xin' ('heart' in Chinese).[3,4] Chicken Xin (cXin) is initially expressed in cardiac progenitor cells of the paired lateral plate mesoderm that forms the primordia of the heart, and its expression continues during all further stages of heart development. A more pronounced lateral expression was observed prior to cardiac looping, while in the looping heart strongest expression was found in the inner curvature. Inactivation of this gene in chick embryos, led to looping defects, abnormal beating behaviour and oedema, and an important role for cXin in heart development was predicted.[4]

Subsequently, a message homologous to cXin was detected in mice and humans. Mammalian Xin colocalizes with N-cadherin in developing cardiomyocytes and with N-cadherin, connexin43, filaminC, and vasodilator-stimulated phosphoprotein (VASP) in the intercalated discs (IDs) of adult hearts.[4,5] IDs mainly consist of a dense plaque, the *area composita*,[6] in which intermediate filaments and actin filaments are tethered to the membrane. A plethora of actin cytoskeleton or intermediate filament binding proteins localize at the ID and their significance for cardiac function has been revealed by animal models[7–9] and human mutations that result in cardiac diseases such as arrhythmogenic right ventricular cardiomyopathy with dilated cardiomyopathy (DCM), and DCM accompanied by disorders in skeletal muscle, skin, or hair.[10] The human Xin-encoding gene maps to chromosome 3p21.2–21.3, at a 'DCM with conduction defect-2' (CMD1E) locus. Further components of IDs are the gap junctions that mainly consist of connexin43 and are responsible for chemical and electrical coupling of cardiomyocytes and the coordination of the rhythmic contraction of the heart.

In an analysis for genes co-expressed with cardiomyopathy-associated (CMYA) genes, five novel genes were identified, including the Xin-encoding gene.[11] This gene was initially designated *CMYA1* (current name: *XIRP1*). In mammals, the *XIRP1* gene exists of two exons, the second of which contains the complete protein-coding region. Splicing of exon 1 to exon 2c and intra-exonic splicing of exon 2a to exon 2c leads to the expression of three isoforms, XinA, XinB, and XinC in humans.[5] A further gene from this group (*CMYA3*) encodes a second Xin-repeat-containing protein. This protein was accordingly named Xin-repeat protein 2 (XIRP2)[2] and the gene renamed *XIRP2*.

Together, these data predict a crucial role for Xin in heart development and cardiac disease. However, mice with a partial deletion of *XIRP1* that still can express XinC are viable, fertile and show normal heart development. They develop cardiac hypertrophy only in later life.[12]

We generated a novel mouse model in which the single coding exon of *XIRP1* is almost entirely deleted. Although these mice do not express any of the three Xin isoforms, they develop normally and exhibit only a mild cardiac phenotype. The slightly more elongated isolated cardiomyocytes of XinABC$^{-/-}$ mice have mislocalized IDs and show a disturbed contractile behaviour upon electrical stimulation. A complete lack of Xin therefore does not lead to major abnormalities of heart development and function, probably due to compensation by the structurally related XIRP2. We also show that cardiac hypertrophy in man is associated with increased expression of XinC, suggesting that this isoform might cause the more severe phenotype in XinAB$^{-/-}$ mice.

2. Methods

2.1 Analysis of Xin isoform expression

To verify that XinC is also expressed in murine hearts, RNA was purified from mouse hearts using the RNeasy fibrous tissue mini kit (Qiagen), and cDNA was prepared using random nonamers and Omniscript reverse transcriptase. Splicing of exon 1 to exon 2c was verified by cloning and sequencing the amplicons that were obtained in PCR experiments using this cDNA as a template and forward primers in exon 1, [P1 (GGACCCAGGAACAGAACAGA) and P2 (GGCTAGACACCCAAAAGCAC)] and a reverse primer in exon 2c [P3 (GGGGTTTCTTTCTTGGAAGC)] (*Figure 1*).

2.2 Generation of XinABC-deficient mice

Two PAC clones (445-F18 and 584-C21) from 129/Sv mouse library RPCI21 (HGMP resource centre, Cambridge, UK) were used for the construction of the targeting vector (*Figure 1C*); and 3.1 kb *Sma*I–*Xho*I and 4.5 kb *Bam*HI–*Xba*I fragments were subcloned into pBS/KS. The blunted *Sma*I/*Xho*I fragment was cloned into *Xho*I-digested vector pWH9, containing an internal ribosomal entry site (IRES) that drives *lacZ* and neomycin gene expression. Subsequently the *Bam*HI–*Xba*I fragment, excised from pBS/KS using *Sal*I and *Not*I, was cloned into the *Sal*I–*Not*I-digested pWH9 vector containing the left arm.

The construct was electroporated into R1 embryonic stem (ES) cells and selected with G-418 as described.[13] Southern blots of *Kpn*I-digested genomic DNA from ES cells were hybridized with a 1.3 kb DNA fragment amplified from genomic DNA (*Figure 1*). Homologous recombinants showed a band of 4.5 kb in addition to the 10 kb wild-type (wt) band. Targeted cells were injected into blastocysts to generate chimeras, which were mated with C57BL/6 females. Genotyping of backcrosses was performed as described above and by PCR using a forward primer in the intron between exons 1 and 2 (CAGGTTC TCCCCTTCTTCCCAG) and primers in exon 2 (CGGCTCCTGAT CTGAGCTGTTG, wt allele) or in the IRES (CCAACTCACAACGT GGCACTGG, recombinant allele). Subsequent analyses were performed in mixed 129/B6 genetic background. The investigation conforms with the Guide for the Care and Use of Laboratory Animals published by the US National Institutes of Health (NIH Publication No. 85-23, revised 1996), and approval for animal studies was granted by the Landesamt für Natur, Umwelt und Verbraucherschutz NRW, registry number 9.93.2.10.35.07.104.

Embryos were harvested (E9, E12.5, and E13.5 dpc), fixed in 4% paraformaldehyde, stained for β-galactosidase, and genotyped. After photography, embryos were embedded in paraffin; and 5 μm sections were cut and haematoxylin and eosin (HE) stained. Cryosections from mouse hearts were stained with anti-Xin and anti-filaminC antibodies as described.[5]

2.3 Tissues, preparation of tissue extracts, western blotting, and immunodetection

Protein extracts from adult mouse hearts were analysed by western blotting essentially as described.[5] Human tissue specimens were obtained from the septum of four normal hearts (two male, two female, age

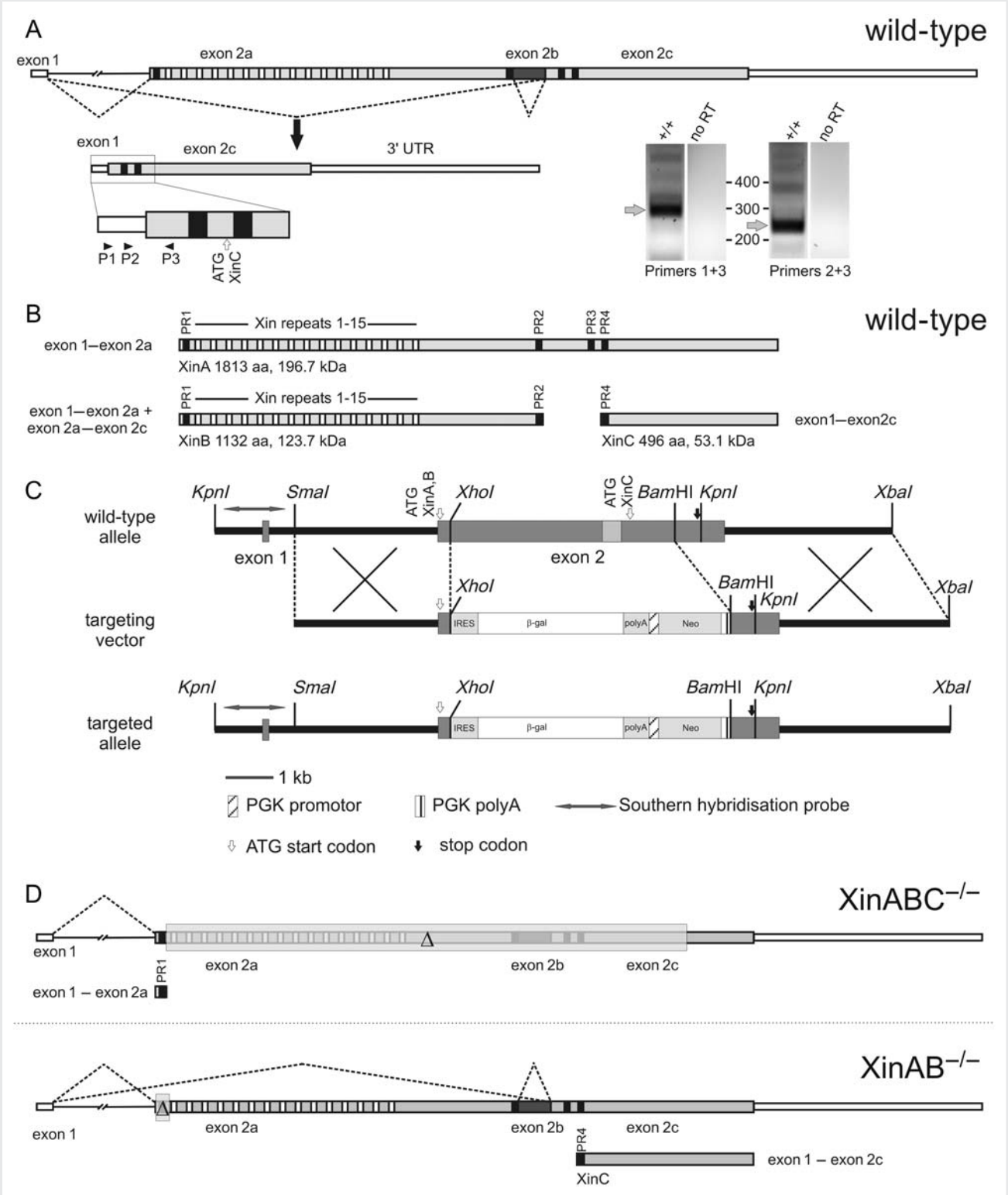

Figure 1 Analysis of Xin isoform expression and effects of two different 'null' mutations. (*A*) Schematic representation of the murine *XIRP1* gene and splicing patterns (dashed lines). The lower part of the figure shows an RT–PCR experiment using RNA from a murine heart as template and the primers marked by arrowheads (P1–P3) to verify that exon 1 can be spliced to exon 2c, confirming expression of XinC. The expected amplicons that were sequenced to verify their identity are marked by grey arrows. (*B*) Protein structure of the three Xin isoforms expressed from the alternatively spliced mRNAs. PR, proline-rich region. (*C*) Schematic diagram showing the strategy of the disruption of *XIRP1* in ES cells. Homologous crossing over leads to the replacement of the major part of exon 2 by the selection marker neomycin and β-galactosidase. (*D*) Comparison of the genotypes of XinABC$^{-/-}$ mice described in this report (upper figure), and XinAB$^{-/-}$ animals and their Xin isoform expression. The parts of the gene deleted in both mouse models are indicated by transparant grey boxes marked Δ. Note that in XinAB$^{-/-}$ mice expression of XinC is not impeded.

5–61 years) and seven hypertrophic cardiomyopathy (HCM) hearts (six male, one female, age 36–73 years). Informed consent was obtained from all subjects. The investigation conforms with the principles outlined in the Declaration of Helsinki. This study was approved by the Ethics Committee of the University of Bochum (registry #1966, 18 July 2002). Western blots using XR1 for murine hearts or a mixture of XR1 and XC3 antibodies to simultaneously detect all human Xin isoforms were prepared essentially as described.[5] Autoradiograms were photographed with a GelDoc System and densitometry was performed using Quantity One Software (BioRad). The rabbit anti-sera MyW17ra[14] and anti-XIRP2/myomaxin[15] were used to detect myomesin and XIRP2, respectively. For establishing XIRP2 and myomesin expression levels, blots were incubated with the respective primary anti-sera and IRDye800-conjugated goat-anti-rabbit Ig enabling quantitative analysis with the Odyssey Infrared Imaging System (Li-Cor, Bad Homburg, Germany).

2.4 Investigation of body parameters

To compare phenotypes of wt and XinABC$^{-/-}$ mice, body weight (BW), heart weight (HW), and tibia length (TL) were analysed in young and old mice. Young mice ($n = 41$) were evaluated at 11.5 weeks $\pm$ 13 days and old mice ($n = 30$) at 83 weeks $\pm$ 14 days.

2.5 Histological and ultrastructural examination of mouse hearts

Hearts of animals of each genotype (young: 12 weeks $\pm$ 8 days, $n = 8$; old: 65 weeks $\pm$ 12 days, $n = 9$) were subjected to retrograde Langendorff-perfusion with EGTA-Tyrode's solution for 20 min and fixed with 4% paraformaldehyde for 24 h. Hearts were then cut into three defined parts and embedded in paraffin; and 5 μm thick sections cut perpendicular to the longitudinal axis were HE stained and the size of the septum and the left cardiac wall were determined by measuring the distances from epicard to endocard at three different positions.

Perivascular fibrosis was analysed on Azan-stained cryosections (6 μm) of cardiac muscle: computerized planimetry (with image-analysis software ImageJ 1.38d) was used to determine the percentage of connective tissue from the total cross-sectional area of the coronary vessels. The area of connective tissue surrounding coronary vessels was normalized to the total area of the vessel. Interstitial fibrosis was investigated in the same sections.

For transmission electron microscopy, cardiac tissue samples of wt and XinABC$^{-/-}$ mice were fixed in 2% glutaraldehyde and 4% paraformaldehyde in 0.1 M sodium cacodylate buffer (pH 7.3) for 60 min at room temperature (RT), post-fixed with 2% unbuffered osmium tetroxide for 60 min at 4°C, and stained *en bloc* with 4% unbuffered uranyl acetate for 90 min at RT. Samples were dehydrated through a graded series of ethanol, cleared in propylene oxide, and embedded in Epoxy resin (Fluka Production GmbH, Buchs, Schweiz). Ultra thin sections were cut with an Ultracut UCT (Leica, Wetzlar, Germany) and stained with 4% unbuffered uranyl acetate for 20 min followed by 2.5% unbuffered lead citrate for 10 min. Specimen were examined with a CM 120 electron microscope equipped with a LaB_6 filament at 80 kV (Philips Electron Optics, Eindhoven, The Netherlands).

2.6 Sarcomere shortening in isolated cardiomyocytes

Isolated ventricular cardiomyocytes were prepared from adult female mice ($n = 15$ of each genotype) and kept in oxygenated Tyrode's solution at 22°C until use. Cells were allowed to attach to laminin-coated microscope slides as described[16] and stimulated externally with 40 V for 0.4 ms. Each series consisted of 20 stimuli at 0.5, 1, 2, 4, 6, 8, and 10 Hz. Sarcomere shortening was recorded using a video imaging system and SarcLen software (Ionoptics, Milton, MA, USA). Fast Fourier transformation was used to analyse striation patterns of sarcomeres. To calculate steady state parameters of shortening, the last five shortenings of each series were averaged and the result of shortening was evaluated.

2.7 Surface ECG and electrophysiological investigation

The surface ECG was monitored continuously. Intracardiac electrograms and transvenous atrial and ventricular stimulation manoeuvres were registered and recorded as previously described.[17–19] Fixed rate and extrastimulus pacing, sinus node recovery time, Wenckebach periodicity, atrial refractory periods and atrioventricular nodal refractory periods (ARP, AVNRP) were evaluated. Ventricular refractory period (VRP) was evaluated similar to ARP by ventricular extrastimulus pacing.

In vivo transvenous electrophysiological investigations were performed in anaesthetized adult XinABC$^{-/-}$ ($n = 16$) and wt ($n = 11$) mice using a 2-French octapolar mouse electrophysiological catheter [eight 0.5 mm circular electrodes; electrode-pair spacing 0.5 mm (Ciber Mouse, NuMed Inc., NY, USA)] that was positioned via the jugular vein in the right atrium and ventricle.[17,19]

2.8 Arrhythmia induction

Atrial fibrillation (AF) was induced by atrial burst stimulation. AF was defined as rapid and fragmented atrial electrograms with irregular AV-nodal conduction for $\geq$1 s.[19,20] Ventricular vulnerability was analogously tested by ventricular burst stimulation for 1 s. Additionally, extrastimulus pacing was performed analogous to human electrophysiological examination (S1S1: 120, 100, and 80 ms followed by up to three extra beats). Ventricular tachycardia (VT) was defined as four or more ventricular ectopic ventricular beats. Number of inducible AF and VT episodes and the probability of arrhythmia induction were analysed.

2.9 Evaluation of morphological parameters of isolated cardiomyocytes

Ventricular cardiomyocytes prepared from five mice of each genotype and attached to laminin-coated microscope slides were fixed with cold (−20°C) methanol (5 min) and acetone (0.5 min). Cell width and length of 70 cells of each animal were measured using an ocular micrometer. Cardiomyocytes were stained with antibodies (see below) to localize ID proteins using standard procedures. The localization of IDs was evaluated statistically.

The following antibodies were used: anti-Xin XR1 and XC3, specific for the N- and C-terminus, respectively;[5] rabbit anti-connexin43 antiserum (generous gift of Professor Willecke); anti pan-cadherin (Sigma); anti-Z-disc titin T12;[21] anti-VASP (generous gift of Professor U. Walther), anti-filamin RR90,[22] anti-desmoplakin DP2.15 (Serotec), anti-SERCA2a (Abcam). Specimens were examined and pictures were acquired using an inverted microscope equipped with fluorescence optics (Nikon Eclipse TE-2000-E) and a cooled CCD camera (DVC Company) and Image Pro Plus software (Media Cybernetics, Surrey, Canada).

2.10 Statistics

Statistic analyses were performed using the one-way and non-parametric ANOVA test with subsequent Bonferroni test. Results are shown as mean $\pm$ standard deviation. Significant differences ($P < 0.05$) are indicated by asterisks: *means a confidence interval of 95% corresponding to a *P*-value less than 0.05; **confidence interval 99%,

P-value less than 0.01; ***confidence interval 99.9%, *P*-value less than 0.001 (*Figure 4*).

3. Results

3.1 Analysis of Xin isoform expression and generation of Xin-depleted mice

Recently a mouse strain was described, in which *XIRP1* was inactivated by homologous recombination.[12] The strategy used eliminates the ATG start codon and replaces a short fragment of the 5' end of the coding region with a *LacZ–Neo* cassette (*Figure 1*). Analysis of human *XIRP1* revealed intra-exonic splice sites within exon 2.[5] We found an identical gene structure in mice and demonstrated by RT–PCR and subsequent sequencing that the predicted splicing of exon 1 to exon 2c occurs *in vivo* (*Figure 1A*), indicating that this mouse strain is a partial knock-out leaving XinC expression intact (*Figure 1B* and *D*). Therefore, we refer to these animals as XinAB$^{-/-}$ mice.

We eliminated all variants of Xin by replacing nearly the entire protein encoding sequence by a cassette containing an IRES the *LacZ* gene and a neomycin resistance gene (*Figure 1C*). Genomic DNA from 360 ES cell clones was analysed for homologous recombination and 17 homologous recombinant clones were identified (*Figure 2A*). Three of those were microinjected into blastocysts to generate chimeric mice in CD1 Foster mice. One of the clones yielded chimeric males and was transmitted through germline. These were crossed with C57BL/6 females to produce heterozygous offspring. Genotyping revealed a Mendelian ratio of genotypes. Western blotting of extracts prepared from cardiac tissue confirmed the complete ablation of Xin in $-/-$ mice, whereas in heterozygous mice expression was considerably reduced (*Figure 2B*). To discriminate this mouse strain from that previously described, we named these animals XinABC$^{-/-}$ mice. XinABC$^{+/-}$ and XinABC$^{-/-}$ mice were viable, fertile, and indistinguishable from their wt littermates.

Immunohistochemistry detected no Xin in the hearts of XinABC$^{-/-}$ animals, whereas the ID localization of filaminC, binding partner of Xin, was not altered (*Figure 2C*). Notably, the IDs in XinABC$^{-/-}$ hearts were more randomly distributed and not mainly localized at the termini of the cardiomyocytes (arrows in *Figure 2C*).

The activity of the *XIRP1* promoter was analysed by staining for β-galactosidase activity in whole mount embryos. In contrast to wt embryos, XinABC$^{+/-}$ and XinABC$^{-/-}$ embryos exhibited β-galactosidase activity. When compared with heterozygous animals, XinABC$^{-/-}$ animals showed a similar distribution but higher activity. In E9 embryos, β-galactosidase activity occurred predominantly in the pericardium. Xin expression was also observed in the somites, indicating involvement of Xin in early skeletal muscle development (*Figure 2D*). Later in development (E12.5) activity of the *XIRP1* promoter was evident in all cross-striated muscles (*Figure 2D* and *E*).

To investigate whether the normal development of the heart in the absence of Xin is accompanied by an upregulation of XIRP2, we analysed the relative expression levels of this protein compared with the M-band component myomesin (*Figure 2F*). Quantification of western blots with the Li-Cor Odyssey Infrared Imaging System showed that expression levels in knock-out animals (0.48 ± 0.12, $n = 8$) were not increased when compared with wt animals (0.50 ± 0.08, $n = 9$).

3.2 Investigation of body parameters

To search for phenotypic differences, HW/TL and HW/BW ratios of old and young wt and XinABC$^{-/-}$ mice were compared. Statistic analyses demonstrated that the BW of aged wt mice was higher than that of XinABC$^{-/-}$ animals. Other parameters did not display any significant differences (Supplementary material online, *Table S1* and *Figure S1*).

3.3 Histological analysis of cardiac tissue

To investigate the effects of the ablation of *XIRP1* on the morphology of the heart, the thickness of the septum and the left ventricular wall were determined using HE-stained sections. No significant differences in the parameters were found (Supplementary material online, *Table S2* and *Figure S2*).

Azan-stained frozen sections revealed that coronary vessels of young XinABC$^{-/-}$ mice exhibited a significantly higher degree of perivascular fibrosis than wt animals (*Figure 3*). This distinction was restricted to young animals, indicating premature fibrosis in the knock-out situation. In contrast, no signs of increased interstitial fibrosis were observed in XinABC$^{-/-}$ mice (Supplementary material online, *Figure S3*).

3.4 Standard ECG and electrophysiological examination

Although global cardiac properties were similar, electrophysiological experiments revealed a significantly shorter HV interval and a trend towards shorter QRS interval in XinABC$^{-/-}$ mice (*Tables 1* and *2*, Supplementary material online, *Figure S4*), indicating a faster conduction velocity of the ventricular-specific conduction system. Atrial and VRPs were equal among the groups and no atrial or VT or fibrillation was induced by programmed or burst stimulation (data not shown). There were more difficulties during catheter placement resulting in more intra-operative deaths in the knock-out group.

3.5 Alterations in the contractile behaviour of isolated cardiac myocytes of XinABC$^{-/-}$ mice

To compare the contractile behaviour of wt and XinABC$^{-/-}$ cardiac cells, the effect of electrical stimulation on sarcomere shortening of isolated ventricular cardiomyocytes was analysed (*Figure 4A*).

Without electrical stimulation, the resting sarcomere length of wt cells was significantly lower than that of XinABC$^{-/-}$ cardiomyocytes (1.814 vs. 1.834 μm; parameter 'baseline'). Sarcomere shortenings were decreased in XinABC$^{-/-}$ mice at low frequencies (*Figure 4B*). At all applied frequencies, XinABC$^{-/-}$ cardiomyocytes exhibited a significantly decreased duration of shortening (*Figure 4F*; parameter 'time-baseline 90'). Conversely, contraction and relaxation velocities differed at least at higher strain (stimulation frequencies above 6 Hz). Thus, XinABC$^{-/-}$ cardiomyocytes contract and relax faster, and with concurrent curve progression

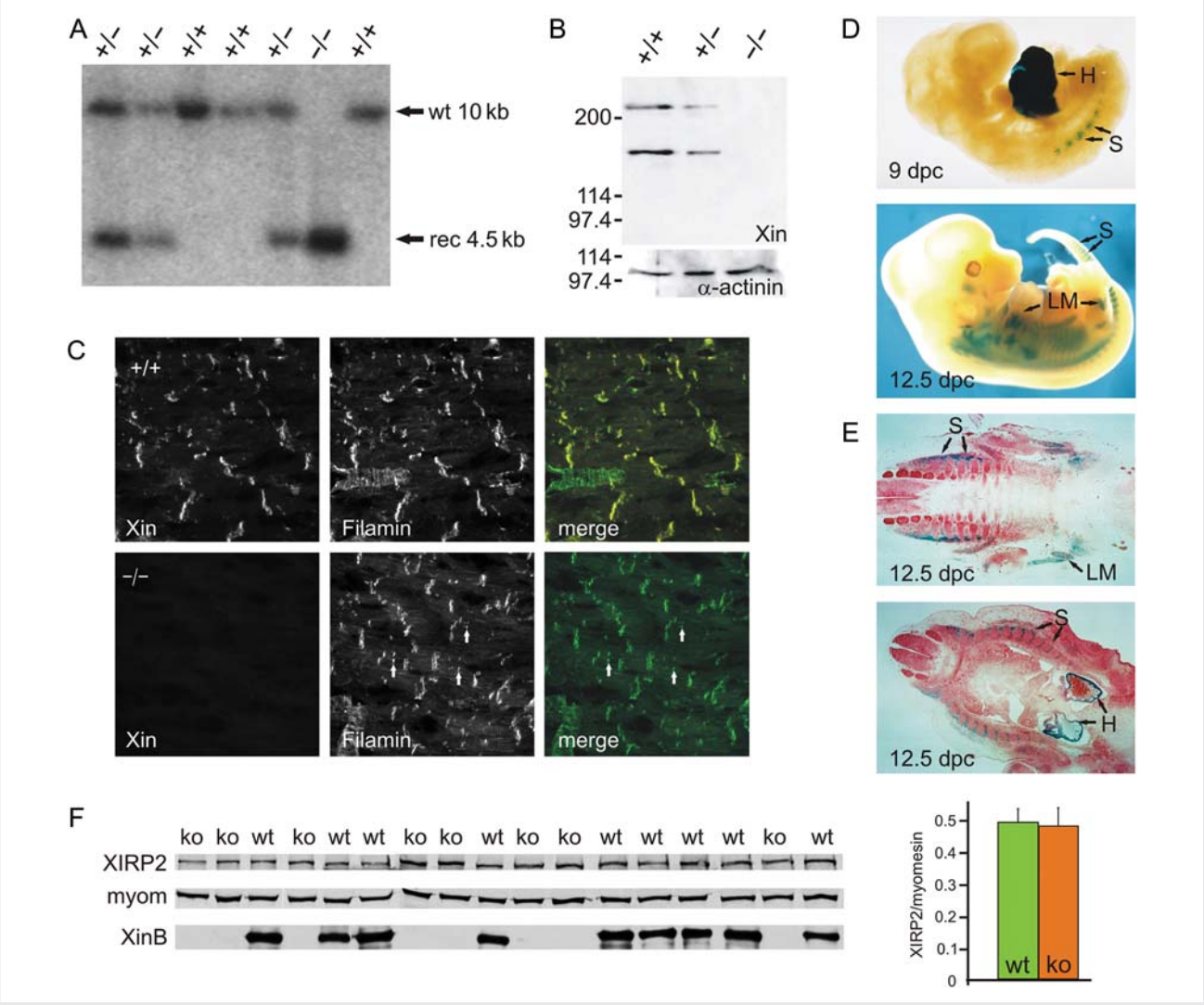

Figure 2 Characterization of mice with a complete Xin-null mutation. (*A*) Southern blot analysis of tail DNA from the progeny of a mating between heterozygous parents. DNAs were digested with *Kpn*I and hybridized with the probe indicated in *Figure 1C*. Analysis of Xin expression in wt, XinABC$^{+/-}$, and XinABC$^{-/-}$ mice by western blotting (*B*) or immunofluorescence assays (*C*) confirm the total absence of the Xin proteins in XinABC$^{-/-}$ mice. Note the unaltered localization of filaminC, an ID component and binding partner of Xin, and the increased lateral localization of IDs in XinABC$^{-/-}$ cardiomyocytes (arrows, see also *Figure 5*). Evaluation of β-galactosidase expression in XinABC$^{-/-}$ embryos (*D*) shows expression in the heart (H) and in somites (S). In 12.5 dpc embryos expression is also observed in all skeletal muscles including those of the limbs (LM). Analysis of sections of a 12.5 dpc XinABC$^{-/-}$ embryo confirms exclusive activity of the *XIRP1* promoter in myogenic cells (*E*). Analysis of XIRP2 expression in wt and XinABC$^{-/-}$ mice by western blotting shows that relative XIRP2 levels are not increased in knock-out mice when compared with the expression level of myomesin (myom). The genotype of the animals analysed was confirmed by staining for XinB (*F*).

(*Figure 4D* and *E*). Accordingly, XinABC$^{-/-}$ cells shorten for a considerably shorter period of time (*Figure 4F*). Data are summarized in *Table 3*.

3.6 Immunolocalization studies of isolated cardiomyocytes reveal alterations in cell dimensions and ID distribution

To check for signs of hypertrophy, the length and width of isolated cardiomyocytes were measured. Whereas the width of the cells did not differ, XinABC$^{-/-}$ cells exhibited a small but significant increase in length (*Figure 5E*).

Since functional analysis of cardiomyocyte contractility revealed differences between wt and XinABC$^{-/-}$ cells, distribution patterns of myofibrillar, sarcoplasmic reticulum (SR), and ID-associated proteins were analysed by immunofluorescence microscopy. Staining for cadherin and connexin43 demonstrated that XinABC$^{-/-}$ cells contained more non-terminal ID-like structures (*Figure 5A* and *B*), while the number of terminally situated IDs was not altered (*Figure 5E* and *Table 4*). Staining of titin did not exhibit disparities between both groups, indicating that abnormal ID

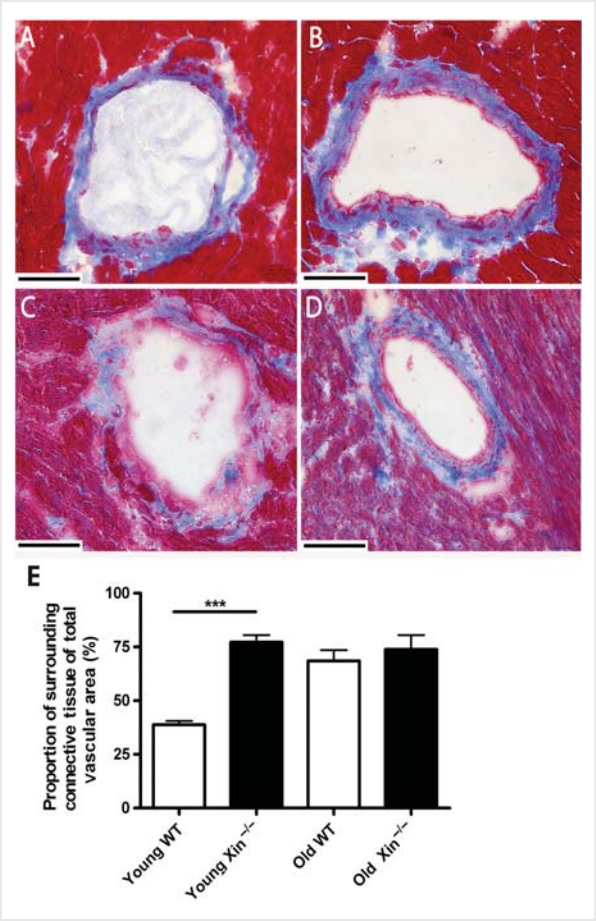

Figure 3 Comparison of perivascular fibrosis in wt and XinABC$^{-/-}$ mice. Cryosections from hearts of young or old wt and XinABC$^{-/-}$ animals were Azan-stained to differentiate connective tissue (light blue) from surrounding tissue (dark red to purple). The micrographs show coronary vessels of young wt (*A*), young XinABC$^{-/-}$ (*B*), old wt (*C*), and old XinABC$^{-/-}$ (*D*) mice. (*E*) Proportion of surrounding connective tissue to the total vascular area in %.

Table 1 Surface ECG parameters

	Wild-type ($n = 11$)	XinABC$^{-/-}$ ($n = 16$)	*P*-value
Heart rate (b.p.m.)	463.8 ± 44.8	466.5 ± 46.4	0.88
P (ms)	18.8 ± 3.0	16.5 ± 3.7	0.96
PQ (ms)	39.5 ± 7.6	44.5 ± 8.8	0.14
QRS (ms)	15.5 ± 2.4	13.5 ± 2.7	0.59
QTc (ms)	89.5 ± 13.1	88.3 ± 9.7	0.79

QTc, rate corrected QT-interval.[18]

distribution is not accompanied by a gross disturbance of myofibril organization (*Figure 5A* and *B*).

Table 2 Intracardiac electrograms and functional electrophysiological testing

	Wild-type ($n = 8$)	XinABC$^{-/-}$ ($n = 7$)	*P*-value
AH (ms)	32.3 ± 5.3	33.4 ± 4.2	0.64
HV (ms)	**12.6 ± 0.9**	**8.7 ± 2.1**	**0.002**
WBP (S1S1, ms)	85.6 ± 8.2	96.1 ± 49.9	0.60
SNRT (ms) at S1S2: 120 ms	173.5 ± 25.7	158.0 ± 20.8	0.38

AH, interval from atrial to His signal; HV, interval from His to first QRS movement in surface ECG; WBP, Wenckebach periodicity; SNRT, sinus node recovery time. Significant differences between wild-type and XinABC$^{-/-}$ animals are printed in bold.

To substantiate this finding, isolated cardiomyocytes were stained with antibodies against ID components filaminC and VASP (two binding partners of Xin) and SERCA2a. VASP (*Figure 5C*) and filaminC (data not shown) showed the expected altered localization in XinABC$^{-/-}$ cells, whereas the sarcomeric localization of filamin was identical to wt cells (data not shown). SERCA2a staining did not reveal any obvious alterations in SR organization (*Figure 5D*). Additional examination of cardiac tissue by electron microscopy indicated that, although no obvious structural changes of sarcomeres or IDs were observed, the characteristic continuous and regularly folded pattern of IDs was frequently interrupted in XinABC$^{-/-}$ mice (*Figure 5F* and *G*).

Thus, the ablation of *XIRP1* leads to an altered distribution of IDs with a normal ultrastructural appearance that is not accompanied by changes in the organization of myofibrils or the distribution of the SR.

3.7 Expression of Xin variants in healthy and hypertrophic human cardiac tissue

Monoclonal antibodies were used to analyse Xin isoform expression in non-failing and hypertrophic human cardiac muscle specimens. The normal myocardium expresses high levels of XinB and lower levels of XinA. Quantitative densitometric analysis of HCM heart specimens demonstrated that XinA:XinB and XinA:α-actinin ratios were altered in hypertrophic human hearts. The expression level of XinA was increased to a level similar to that of XinB, while the amount of XinB remained constant (*Figure 6*). Most interestingly, XinC is upregulated in all HCM samples (*Figure 6*), suggesting that this isoform might be involved in the pathogenesis of HCM.

4. Discussion

Cross-striated muscle cells undergo extensive actin cytoskeleton remodelling during early morphogenesis and hypertrophic growth. These morphogenetic processes involve the reorganization of thin filaments from irregular length and random orientation in stress fibre-like structures to bundles of filaments of uniform length organized at myofibrillar Z-discs. The latter involves

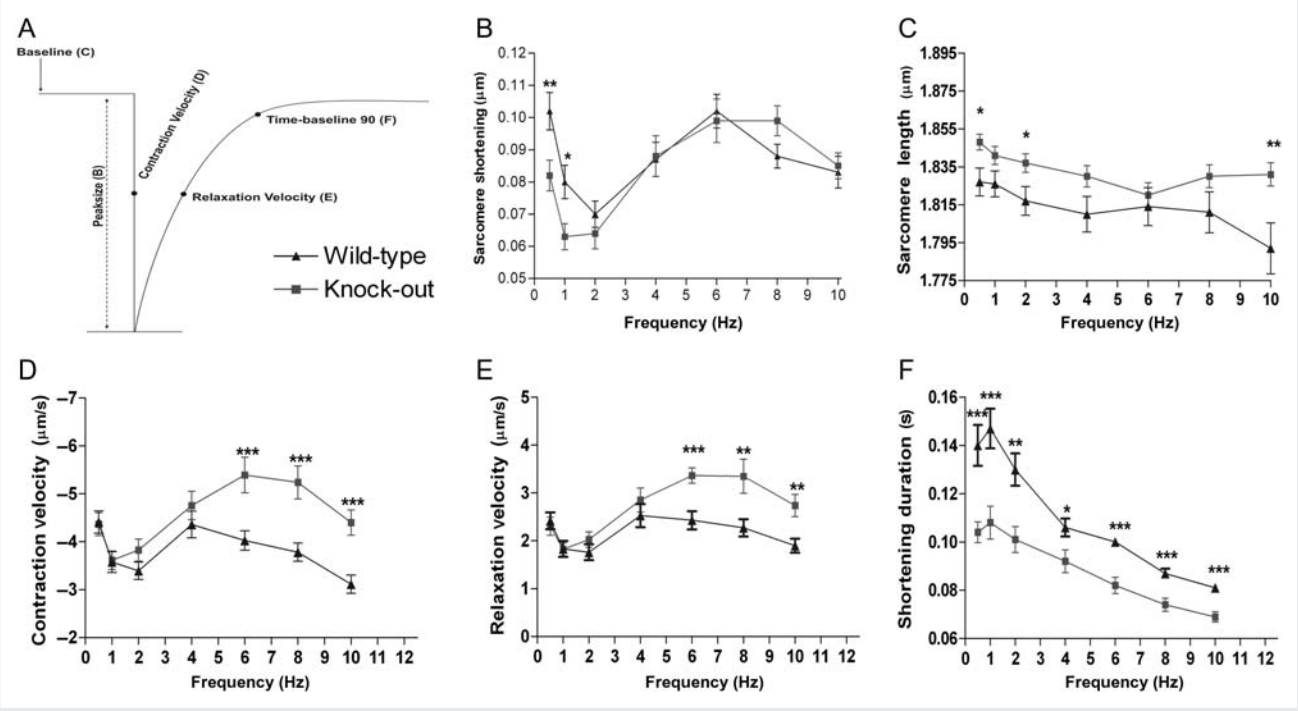

Figure 4 Sarcomere shortening of wt and XinABC$^{-/-}$ cardiomyocytes upon external stimulation. Cardiomyocytes of wt and XinABC$^{-/-}$ mice (n=15; age 12 weeks) were isolated and sarcomere shortenings were recorded. The parameters are highlighted in a typical graph in (*A*). Note that in XinABC$^{-/-}$ cells, resting sarcomere length (*C*) is significantly increased, peak shortening at 0.5–1 Hz (*B*), and duration of shortening (*F*) were lowered, and shortening (*D*) and relengthening velocities (E) were accelerated above 4 Hz. Statistically significant differences are emphasized by asterisks (see Section 2.10).

connections to neighbouring myofibrils and to the extracellular matrix or adjacent cells via specialized membrane complexes. Such gross structural changes require the stringent control and coordination of the activity of several actin-binding proteins that control polymerization dynamics, filament length, and three-dimensional arrangement of filaments.

Xin has properties that make it an ideal candidate for a key role in controlling cardiac morphogenesis. Most importantly, suppression of Xin expression in chick embryos leads to several kinds of cardiac malformations[4] and partial ablation of the gene results in cardiac hypertrophy and conduction defects in mice.[12] Its localization at adherens junctions of muscle cells[23] and binding to actin filaments,[1,2] β-catenin,[24] filaminC, and Mena/VASP[5] imply a role as an adapter protein involved in actin cytoskeleton remodelling.

Our elucidation of the splicing pathway of the *XIRP1* gene implies expression of the XinC isoform in the previously described XinAB$^{-/-}$ mice.[12] Here, we report the characterization of mice in which *XIRP1* has been ablated by a fundamentally different strategy. Interestingly, and somewhat surprisingly, ablation of all Xin isoforms in our XinABC$^{-/-}$ animals resulted in an even milder phenotype with essentially no anatomical alterations (Supplementary material online, *Figure S1*). A lack of increase in the expression levels of cardiac hypertrophy markers (ANP, BNP, myosin heavy chain *MYH7*; unpublished results) is in accordance with equal cardiac wall and septum thickness (Supplementary material online, *Figure S2*) and an only slightly elevated cell length (*Figure 5E*). A conspicuous feature of XinABC$^{-/-}$ cardiomyocytes is, however, a generalized change of ID distribution (*Figure 5B, C, G*) and alterations in contractile behaviour (*Figure 4*). In contrast, in XinAB$^{-/-}$ mice only aberrant, laterally located connexin43 was detected. Most other ID markers such as α-catenin, desmoplakin, and plakoglobin were partly expressed at lower levels, but not mislocalized.[12]

The moderate changes in electrophysiological properties in XinABC$^{-/-}$ hearts point towards a minor impact of Xin-deficiency on gross electrical cardiac homeostasis. However, more gap junctions were observed in isolated Xin knock-out cardiomyocytes, especially in form of side-to-side contacts. Increased numbers of gap junctions in cells of the conduction system might lead to a decreased intercellular resistance explaining the elevated conduction velocity. Despite this potentially arrhythmogenic distribution of connexin43, there was no electrophysiological evidence for enhanced atrial or ventricular vulnerability. Likewise, these alterations do not translate into obvious functional restraints, which may be entirely different upon cardiac stress.

We have compared contractility parameters of isolated cardiomyocytes under strain exerted by electrical stimulation. The slightly longer resting sarcomere length of XinABC$^{-/-}$ cells may be caused by lower concentrations of free Ca^{2+} due to a slight imbalance of activities of SERCA2a and the sodium/calcium exchanger. In line with this assumption, peak size (a parameter for sarcomere shortening) is significantly smaller at low frequencies

Table 3 Contractility measurements of isolated cardiac myocytes

Parameters	Stimulation frequency (Hz)													
	0.5		1		2		4		6		8		10	
	Wt	XinABC$^{-/-}$	Wt	XinABC$^{-/-}$	Wt	XinABC$^{-/-}$	Wt	XinABC$^{-/-}$	Wt	XinABC$^{-/-}$	Wt	XinABC$^{-/-}$	Wt	XinABC$^{-/-}$
Baseline (μm)	**1.827**	**1.848**	1.826	1.841	**1.817**	**1.837**	1.810	1.830	1.814	1.820	1.811	1.830	**1.792**	**1.831**
SD	**0.063**	**0.036**	0.061	0.037	**0.063**	**0.039**	0.069	0.041	0.076	0.042	0.075	0.044	**0.087**	**0.043**
n	**74**	**74**	79	61	**69**	**64**	54	53	58	40	49	53	**42**	**49**
Peak size (μm)	**0.102**	**0.080**	**0.080**	**0.063**	0.070	0.064	0.087	0.088	0.102	0.099	0.088	0.099	0.083	0.085
SD	**0.050**	**0.041**	**0.046**	**0.033**	0.034	0.039	0.039	0.047	0.040	0.041	0.030	0.034	0.032	0.028
n	**74**	**74**	**79**	**67**	69	66	54	55	58	37	65	53	42	49
s Contract (μm/s)	4.409	4.364	3.573	3.611	3.390	3.821	4.358	4.753	**4.023**	**5.390**	**3.779**	**5.236**	**3.112**	**4.397**
SD	2.000	2.048	1.928	1.596	1.503	1.861	2.052	2.134	**1.544**	**2.399**	**1.531**	**2.512**	**1.242**	**1.843**
n	74	74	7	69	69	66	54	53	**58**	**42**	**65**	**53**	**42**	**49**
s Relax (μm/s)	2.147	2.305	1.831	1.821	1.761	2.027	2.528	2.852	**2.430**	**3.365**	**2.271**	**3.350**	**1.898**	**2.738**
SD	1.503	1.538	1.496	1.064	1.371	1.298	1.768	1.829	**1.436**	**1.832**	**1.451**	**2.585**	**0.942**	**1.616**
n	74	66	79	61	69	64	54	53	**58**	**126**	**65**	**53**	**42**	**49**
t-bl90 (s)	**0.140**	**0.104**	**0.147**	**0.108**	**0.130**	**0.101**	**0.106**	**0.092**	**0.100**	**0.082**	**0.087**	**0.074**	**0.081**	**0.069**
SD	**0.073**	**0.073**	**0.073**	**0.730**	**0.056**	**0.056**	**0.027**	**0.027**	**0.014**	**0.014**	**0.016**	**0.016**	**0.012**	**0.012**
n	**74**	**74**	**79**	**79**	**69**	**69**	**54**	**54**	**58**	**58**	**65**	**65**	**42**	**42**

Parameters measured are indicated in *Figure 4A*. s Contract indicates contraction velocity and s Relax gives relaxation velocity. Significant differences between wild-type and XinABC$^{-/-}$ animals are printed in bold.

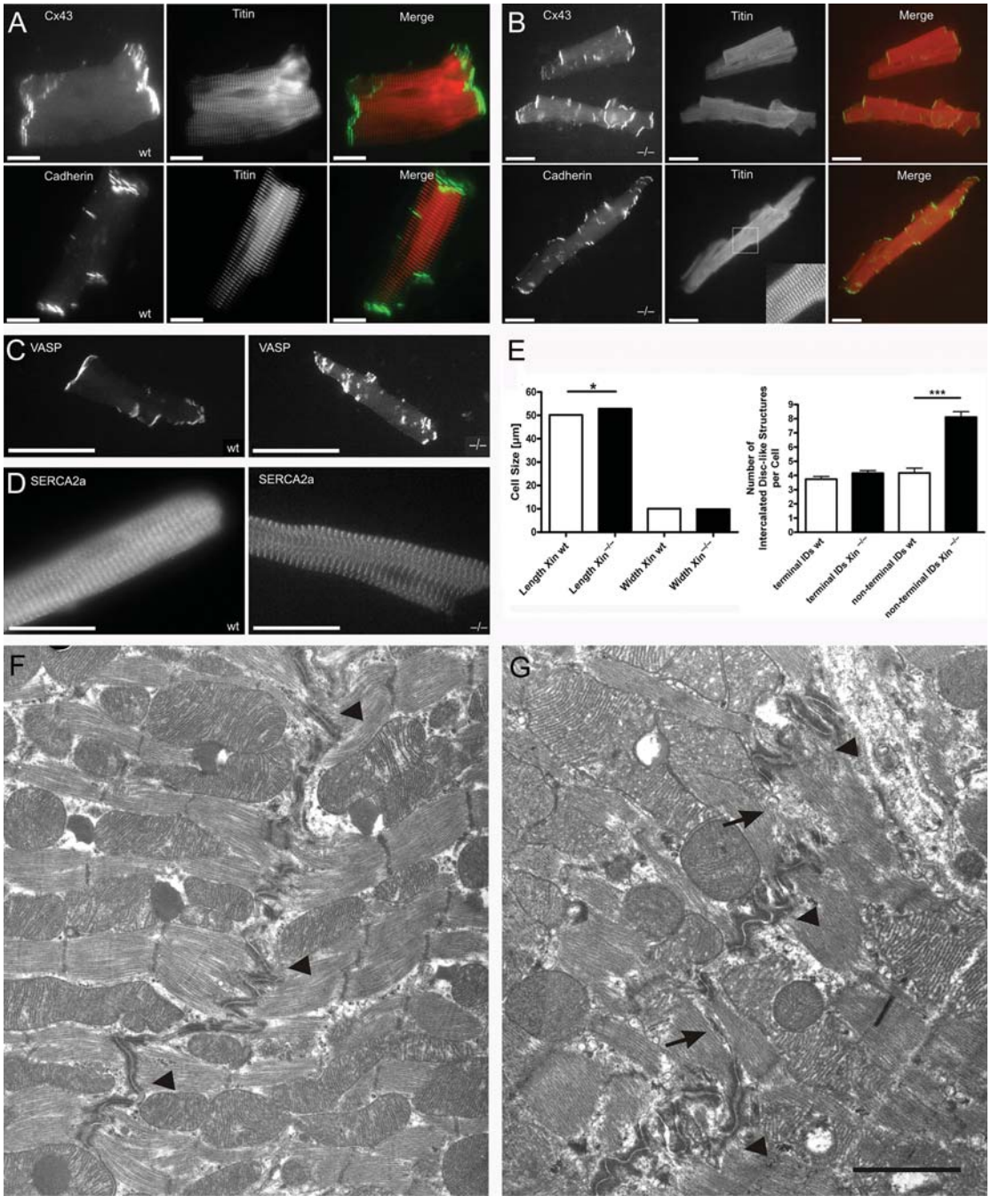

Figure 5 Microscopical evaluation and immunolocalization of myofibrillar, ID and SR proteins in isolated cardiomyocytes and ultrastructure of heart muscle tissue. Isolated cardiomyocytes (n=70/genotype) were stained with the indicated antibodies as markers for IDs (connexin43, cadherin, VASP), myofibrils (titin) or the sarcoplasmatic reticulum (SERCA2a). Staining of wild-type (wt) and XinABC$^{-/-}$ ($-/-$) cardiac myocytes with all ID antibodies demonstrated major alterations in the distribution of IDs (gap junctions and adherens junctions) in XinABC$^{-/-}$ mice. Note that VASP, a direct binding partner of Xin, is still localized to the abnormally distributed IDs in the absence of Xin (*C*). The organization of myofibrils (*A*, *B* titin) and the sarcoplasmatic reticulum (*D*) is not disturbed in knock-out cells. Quantitative analysis confirmed the higher relative number of laterally localized IDs in $-/-$ cells and revealed that XinABC$^{-/-}$ cardiac myocytes were slightly but significantly longer than wt cells (*E*). Electron micrographs displaying ultra-thin sections of cardiac tissue from wt (*F*) and XinABC$^{-/-}$ mice (*G*) reveal significant differences of ID structures (arrowheads). The continuous and regularly folded pattern of IDs characteristic for wt hearts (*F*) was frequently interrupted in XinABC$^{-/-}$ mice (*G*) by gaps which span a distance of about 1 µm and lack the typical folding. Scale bars: 20 (*A*), 50 (*B*), 110 (*C*), 30 (*D*), and 1 µm (*F* and *G*).

Table 4 ID distribution and cell dimensions of isolated cardiomyocytes

Genotype	No. of terminal IDs	No. of lateral IDs	Length (μm)	Width (μm)
Wt	3.79 ± 1.255 ($n = 46$)	4.174 ± 2.312 ($n = 46$)	50.1732 ± 2.580 ($n = 250$)	10.090 ± 0.09108 (n=250)
XinABC$^{-/-}$	4.155 ± 1.424 ($n = 58$)	**8.103 ± 2.995*** ($n = 58$)	**52.810 ± 3.1086*** ($n \geq 400$)	9.801 ± 0.9207 ($n = 400$)

Statistically significant differences are emphasized by asterisks (see Section 2.10) and by bold print.

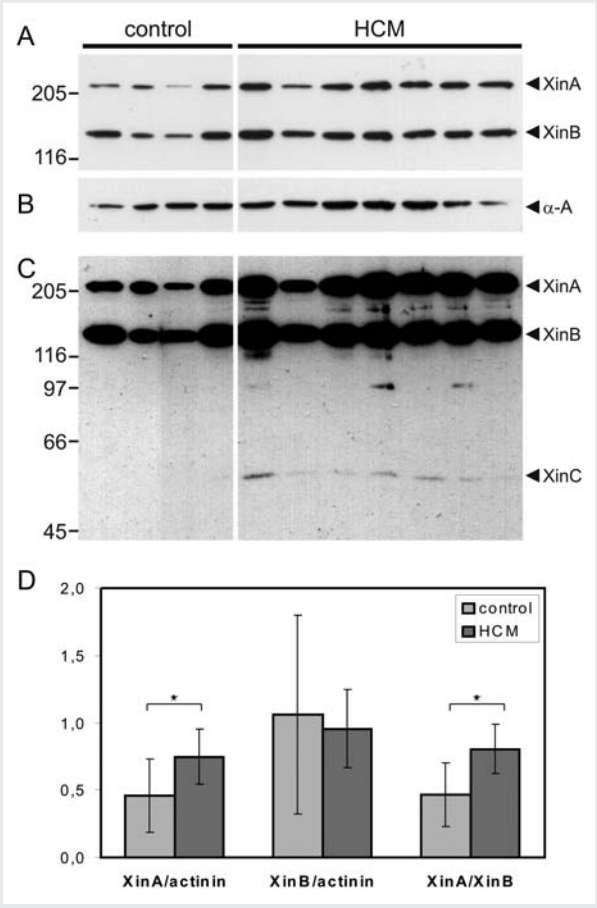

Figure 6 Analysis of the expression patterns of Xin isoforms in the normal and hypertrophic human heart. Total protein extracts from normal (control) and HCM hearts were separated and transferred to nitrocellulose. (*A* and *C*) Autoradiograms of blots (short and long exposure, respectively) incubated with a mixture of antibodies that detect all Xin isoforms. (*B*) The same blot stained for sarcomeric α-actinin (α-A) that was used as reference. (*D*) The ratios XinA: α-actinin, XinB: α-actinin, and XinA:XinB, as determined by densitometry. Bars indicate standard deviation. Note that in HCM samples the ratios XinA:XinB and XinA:α-actinin are significantly increased (*D*) and that the XinC isoform is detected only in HCM samples (*C*).

and the duration of shortening is decreased (*Figure 4*). These alterations must be subtle, since SERCA2a localization was not significantly different in XinABC$^{-/-}$ mice.

The most probable primary reason for the milder than anticipated phenotypes of both knock-out lines is functional compensation by XIRP2[2] (also called myomaxin[15] or mXinβ[12]), whose expression is increased in XinAB$^{-/-}$ mice[12] but not affected in XinABC$^{-/-}$ mice (this work). XIRP2 is highly related to Xin in terms of primary structure. Similar binding properties were shown for F-actin[2] and predicted for β-catenin, Mena/VASP, and filaminC[25] (unpublished results). These findings further suggest that the expression of XinC in XinABC$^{-/-}$ mice may explain their more pronounced phenotype. Instead, it seems detrimental for cardiac performance. Accordingly, analysis of normal and hypertrophic human cardiac samples revealed XinC protein only in hypertrophic tissues (*Figure 6*). To understand these effects more precisely, it will be important to better characterize the role of this Xin isoform in the normal and diseased heart and to identify ligands apart from filaminC that specifically bind XinC.

Nevertheless, it remains puzzling why in Xin knock-out mice the effects on cardiac development (and performance) are only minor when compared with Xin knock-down by antisense inhibition in the chicken embryos. A recent analysis of the genes encoding Xin-repeat proteins in the vertebrate phylum may provide an answer to this paradox: while fish and mammalian genomes harbour three and two homologous genes, respectively, only a single gene has been discovered in the chicken genome.[25] This opens the intriguing possibility that the lack of a second Xin-repeat gene in birds precludes the functional compensation that obviously occurs in mice.

Supplementary material

Supplementary Material is available at *Cardiovascular Research* online.

Acknowledgements

We gratefully acknowledge the invaluable help of Professor R. Fässler in producing this mouse strain. We thank Mrs K. Bois, B. Mai, A Guhlan, H. Bock, U. Romerscheidt-Fuß, U. Kukulies, C. Hennes, and Mr C. Preiss for technical assistance, Professor U. Walter (University of Würzburg, Germany) and Professor K. Willecke for generous donation of antibodies, Dr L. Heukamp for paraffin-embedding, sectioning, and staining of cardiac tissue specimens, and Dr. A. Shakeri-Garakani for help with genotyping of ES cells. Mrs A. Linnemann is thanked for help with the quantification of protein expression.

Conflict of interest: none declared.

Funding

This study was supported by a grant from the Deutsche Forschungsgemeinschaft (grant number FU339/5-1 to D.O.F. and R.M.). D.O.F. and P.F.M.V. are supported by a grant from the German network on muscular dystrophies (MD-NET) funded by the German Ministry of Education and Research (BMBF, Bonn, Germany).

References

1. Cherepanova O, Orlova A, Galkin VE, van der Ven PFM, Fürst DO, Jin JP *et al.* Xin-repeats and nebulin-like repeats bind to F-actin in a similar manner. *J Mol Biol* 2006;**356**:714–723.
2. Pacholsky D, Vakeel P, Himmel M, Löwe T, Stradal T, Rottner K *et al.* Xin repeats define a novel actin-binding motif. *J Cell Sci* 2004;**117**:5257–5268.
3. Wang DZ, Hu X, Lin JLC, Kitten GT, Solursh M, Lin JJC. Differential displaying of mRNAs from the atrioventricular region of developing chicken hearts at stages 15 and 21. *Front Biosci* 1996;**1**:a1–a15.
4. Wang DZ, Reiter RS, Lin JL, Wang Q, Williams HS, Krob SL *et al.* Requirement of a novel gene, Xin, in cardiac morphogenesis. *Development* 1999;**126**:1281–1294.
5. van der Ven PFM, Ehler E, Vakeel P, Eulitz S, Schenk JA, Milting H *et al.* Unusual splicing events result in distinct Xin isoforms that associate differentially with filamin C and Mena/VASP. *Exp Cell Res* 2006;**312**:2154–2167.
6. Franke WW, Borrmann CM, Grund C, Pieperhoff S. The area composita of adhering junctions connecting heart muscle cells of vertebrates. I. Molecular definition in intercalated disks of cardiomyocytes by immunoelectron microscopy of desmosomal proteins. *Eur J Cell Biol* 2006;**85**:69–82.
7. Kostetskii I, Li J, Xiong Y, Zhou R, Ferrari VA, Patel VV *et al.* Induced deletion of the N-cadherin gene in the heart leads to dissolution of the intercalated disc structure. *Circ Res* 2005;**96**:346–354.
8. Radice GL, Rayburn H, Matsunami H, Knudsen KA, Takeichi M, Hynes RO. Developmental defects in mouse embryos lacking N-cadherin. *Dev Biol* 1997;**181**:64–78.
9. Ruiz P, Brinkmann V, Ledermann B, Behrend M, Grund C, Thalhammer C *et al.* Targeted mutation of plakoglobin in mice reveals essential functions of desmosomes in the embryonic heart. *J Cell Biol* 1996;**135**:215–225.
10. Awad MM, Calkins H, Judge DP. Mechanisms of disease: molecular genetics of arrhythmogenic right ventricular dysplasia/cardiomyopathy. *Nat Clin Pract Cardiovasc Med* 2008;**5**:258–267.
11. Walker MG. Pharmaceutical target identification by gene expression analysis. *Mini Rev Med Chem* 2001;**1**:197–205.
12. Gustafson-Wagner EA, Sinn HW, Chen YL, Wang DZ, Reiter RS, Lin JL *et al.* Loss of mXinalpha, an intercalated disk protein, results in cardiac hypertrophy and cardiomyopathy with conduction defects. *Am J Physiol Heart Circ Physiol* 2007;**293**:H2680–H2692.
13. Fassler R, Meyer M. Consequences of lack of beta 1 integrin gene expression in mice. *Genes Dev* 1995;**9**:1896–1908.
14. Obermann WMJ, Gautel M, Steiner F, van der Ven PFM, Weber K, Fürst DO. The structure of the sarcomeric M band: localization of defined domains of myomesin, M-protein, and the 250-kD carboxy-terminal region of titin by immunoelectron microscopy. *J Cell Biol* 1996;**134**:1441–1453.
15. Huang HT, Brand OM, Mathew M, Ignatiou C, Ewen EP, McCalmon SA *et al.* Myomaxin is a novel transcriptional target for MEF2A that encodes a Xin related alpha-actinin interacting protein. *J Biol Chem* 2006;**281**:39370–39379.
16. Tiemann K, Weyer D, Djoufack PC, Ghanem A, Lewalter T, Dreiner U *et al.* Increasing myocardial contraction and blood pressure in C57BL/6 mice during early postnatal development. *Am J Physiol Heart Circ Physiol* 2003;**284**:H464–H474.
17. Kreuzberg MM, Schrickel JW, Ghanem A, Kim JS, Degen J, Janssen-Bienhold U *et al.* Connexin30.2 containing gap junction channels decelerate impulse propagation through the atrioventricular node. *Proc Natl Acad Sci USA* 2006;**103**:5959–5964.
18. Mitchell GF, Jeron A, Koren G. Measurement of heart rate and Q-T interval in the conscious mouse. *Am J Physiol Heart Circ Physiol* 1998;**274**:H747–H751.
19. Schrickel JW, Brixius K, Herr C, Clemen CS, Sasse P, Reetz K *et al.* Enhanced heterogeneity of myocardial conduction and severe cardiac electrical instability in annexin A7-deficient mice. *Cardiovasc Res* 2007;**76**:257–268.
20. Schrickel JW, Bielik H, Yang A, Schimpf R, Shlevkov N, Burkhardt D *et al.* Induction of atrial fibrillation in mice by rapid transesophageal atrial pacing. *Basic Res Cardiol* 2002;**97**:452–460.
21. Fürst DO, Osborn M, Nave R, Weber K. The organization of titin filaments in the half-sarcomere revealed by monoclonal antibodies in immunoelectron microscopy: a map of ten nonrepetitive epitopes starting at the Z line extends close to the M line. *J Cell Biol* 1988;**106**:1563–1572.
22. van der Ven PFM, Obermann WMJ, Lemke B, Gautel M, Weber K, Fürst DO. Characterization of muscle filamin isoforms suggests a possible role of γ-filamin/ABP-L in sarcomeric Z-disc formation. *Cell Motil Cytoskeleton* 2000;**45**:149–162.
23. Sinn HW, Balsamo J, Lilien J, Lin JJ. Localization of the novel Xin protein to the adherens junction complex in cardiac and skeletal muscle during development. *Dev Dyn* 2002;**225**:1–13.
24. Choi S, Gustafson-Wagner EA, Wang Q, Harlan SM, Sinn HW, Lin JL *et al.* The intercalated disc protein, mXinalpha, is capable of interacting with beta-catenin and bundling actin filaments. *J Biol Chem* 2007;**282**:36024–36036.
25. Grosskurth SE, Bhattacharya D, Wang Q, Lin JJ. Emergence of Xin demarcates a key innovation in heart evolution. *PLoS ONE* 2008;**3**:e2857.